An Assessment of the Effects of Bathymetric Changes Associated with Sand and Gravel Mining on Tidal Circulation in the Lower Bay of New York Harbor

Kuo-Chuin Wong
R.E. Wilson

marine sciences research center
state university of new york

SPECIAL REPORT 18

sea grant
new york
institute
suny and cornell

REFERENCE 79-1

MARINE SCIENCES RESEARCH CENTER
STATE UNIVERSITY OF NEW YORK
STONY BROOK, NEW YORK 11794

AN ASSESSMENT OF THE EFFECTS OF BATHYMETRIC CHANGES ASSOCIATED WITH SAND AND GRAVEL MINING ON TIDAL CIRCULATION IN THE LOWER BAY OF NEW YORK HARBOR

Kuo-Chuin Wong and Robert E. Wilson

January 1979

This study was funded by the New York Sea Grant Institute through a contract with New York State Office of General Services, and by SUNY

Special Report 18

Reference 79-1

Approved for Distribution

JR Schubel

J. R. Schubel, Director

TABLE OF CONTENTS

		Page
	List of Figures	ii
	List of Tables	iii
	Abstract	1
I.	Introduction	2
II.	Methodology	4
III.	Results	11
IV.	Conclusions	21
V.	Acknowledgement	22
VI.	Notation	23
VII.	References	24

LIST OF FIGURES

		Page
Figure 1	Resource map for the Lower Bay of New York Harbor indicating median particle diameter (mm) for surface sediment samples [from Kastens et al., 1978].....	3
Figure 2a	Finite element grid for the Lower Bay of New York Harbor indicating the numbers of selected nodes and elements discussed in text.....	5
2b	Finite element grid for the Lower Bay of New York Harbor indicating the eight regions of hypothetical mining (shaded).....	6
Figure 3a	Computed tidal current vectors for existing bathymetry (NOS hydrographic chart No. 12327, 70th Ed., July 1977) for maximum ebb at Sandy Hook.....	7
3b	Computed tidal current vectors for existing bathymetry (NOS hydrographic chart No. 12327, 70th Ed., July 1977) for maximum flood at Sandy Hook.....	8
Figure 4	Comparison of tidal current vectors near maximum ebb at Sandy Hook computed for existing bathymetry (dashed arrows) and altered bathymetry (solid arrows) for (a) small region mined near Sandy Hook, (b) large region mined near Sandy Hook (see Figure 2b).....	12
Figure 5	Comparison of tidal current vectors near maximum ebb at Sandy Hook computed for existing bathymetry (dashed arrows) and altered bathymetry (solid arrows) for (a) small region mined near Rockaway Point, (b) large region near Rockaway Point (see Figure 2b).....	13
Figure 6	Comparison of tidal current vectors near maximum ebb at Sandy Hook computed for existing bathymetry (dashed arrows) and altered bathymetry (solid arrows) for (a) small region, (b) intermediate size region, (c) very large region mined near Staten Island (see Figure 2b).....	14
Figure 7	Comparison of tidal elevation along Staten Island at node 10 (Figure 2a) computed for existing bathymetry (dashed lines) and altered bathymetry (solid lines) for (a), (b) small and large region mined near Sandy Hook; (c), (d) small and large region mined near Rockaway Point; (e), (f), (g) small, intermediate and very large region mined near Staten Island; (h) very large region mined in Raritan Bay (see Figure 2b). Tidal datum is discussed in text.....	15

LIST OF FIGURES (continued)

		Page
Figure 8	Comparison of tidal elevation along Staten Island at node 116 (Figure 2a) computed for existing bathymetry (dashed lines) and altered bathymetry (solid lines) for (a), (b) small and large region mined near Sandy Hook; (c), (d) small and large region mined near Rockaway Point; (e), (f), (g) small, intermediate and very large region mined near Staten Island; (h) very large region mined in Raritan Bay (see Figure 2b). Tidal datum is discussed in text.....	16
Figure 9	Two-dimensional potential flow past a semicircular ditch (a); coordinate system defining the coaxal coordinate $\varepsilon = \theta_1 - \theta_2$ and $\eta = \ln(r_2/r_1)$ used to describe flow (b) (see text).....	19

LIST OF TABLES

		Page
Table 1.	Amplitude and phase of M_2 tide specified at the open boundaries.....	9
Table 2.	Comparison of the magnitude of tidal current vectors for maximum ebb at Sandy Hook computed for existing bathymetry and altered bathymetry. See Figure 2 for relative positioning of elements and mined regions. Abbreviations used below for geographic locations: SH- Sandy Hook, RP - Rockaway Point, SI - Staten Island.....	17

ABSTRACT

Present sand and gravel mining operations within the Lower Bay of New York Harbor are restricted to the east bank of Ambrose Channel and to the vicinity of Chapel Hill North Channel because of the concern than mining in other areas might adversely affect water quality and shore erosion. As part of an evaluation of environmental affects associated with expanded sand and gravel mining we have simulated numerically tidal circulation patterns and tidal elevations in Lower Bay for a number of altered bathymetries corresponding to hypothetical mining operations. Results suggest that tidal currents will decelerate over the mined region and accelerate outside of them, and that the tidal stream will be deflected towards the region. It is also clear that the mining near the mouth of the Bay could increase tidal range along Staten Island substantially.

INTRODUCTION

Research having as an overall goal the evaluation of environmental effects of sand and gravel mining in New York Harbor is presently being sponsored by New York State Sea Grant Institute. Stated goals of this research include an assessment of the environmental impacts that would result from varied and expanded sand and gravel mining activities including different rates and patterns of removal in different parts of the Harbor. Present mining operations within the Harbor are restricted to the east bank of Ambrose Channel and to the Chapel Hill North Channel (Figure 1). These restrictions were imposed largely because of concern of the New York Department of Environmental Conservation that acute ecological impacts of mining in other areas would be greater and that changes in the bathymetry might adversely affect water quality and shore erosion. There is no scientific basis for these assertions and restriction of mining to the present area has diminished the economic value of recovered sand because it is suitable only as fill. In other areas of the Harbor aggregate grade material does occur (Figure 1) and it should be utilized if no persistent adverse effects would occur.

Fundamental to an assessment of the environmental impacts which would result from varied or expanded mining activity is a determination of the changes in tidal circulation and tidal elevation in the Lower Bay which would be produced by the changes in bathymetry. Using a numerical model, we have simulated tidal circulation patterns and tidal elevations in the Bay for a number of altered bathymetries corresponding to hypothetical sand and gravel mining operations. We have attempted to assess the effects of mining activities on tidal circulation and tidal elevation in light of these simulations. These assessments should be useful for the development of an effective management plan for sand and gravel mining in Lower Bay.

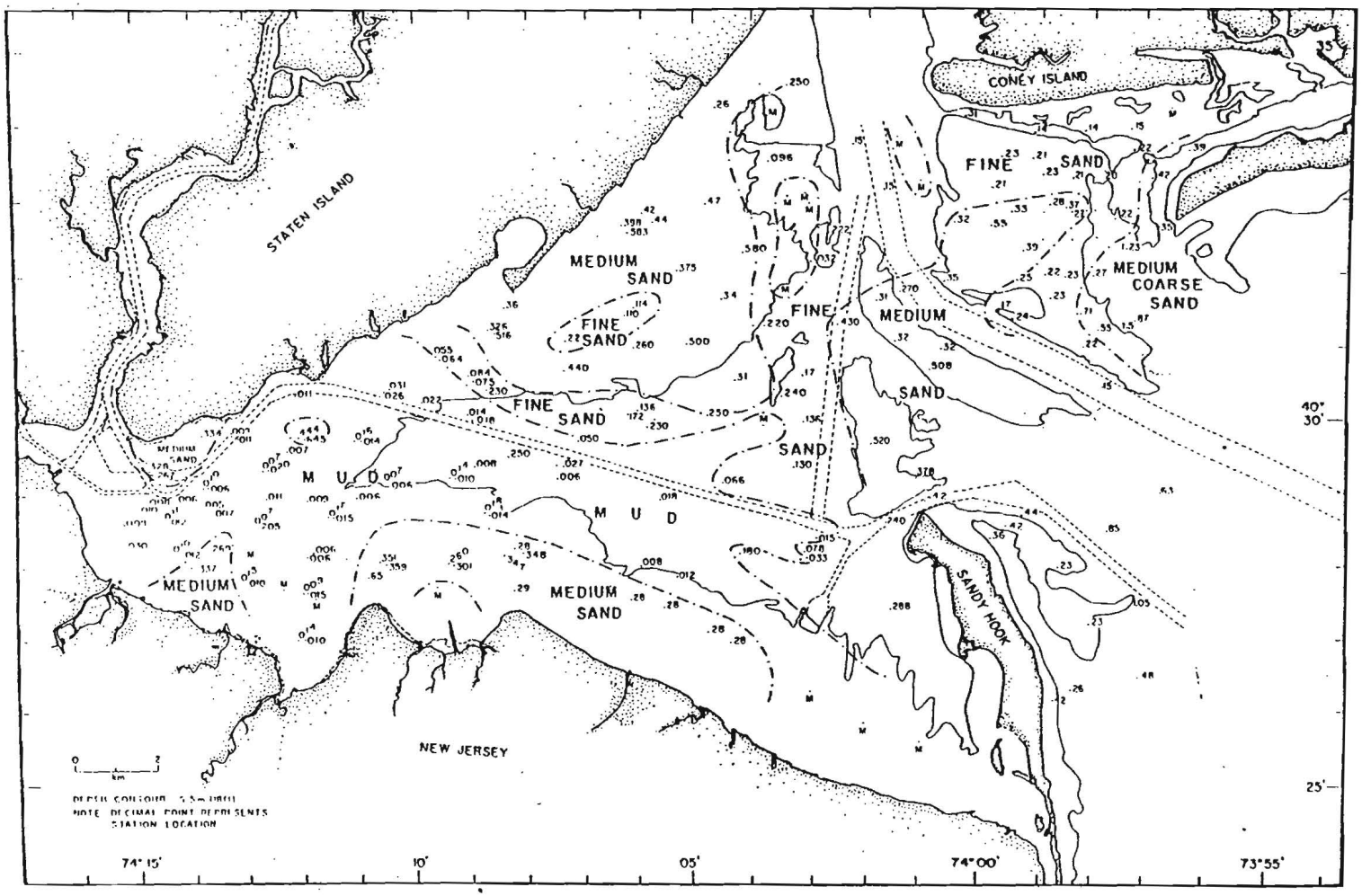

Figure 1 Resource map for the Lower Bay of New York Harbor indicating median particle diameter (mm) for surface sediment samples [from Kastens et al., 1978].

METHODOLOGY

The model used here for the prediction of tidal circulation patterns and tidal elevations in Lower Bay is a finite element hydrodynamical-numerical model CAFE-1 developed under the Sea Grant program at the Massachusetts Institute of Technology [Connor *et al.*, 1973; Wang and Connor, 1975; Pagenkopf *et al.*, 1976]. It is based on vertically integrated continuity and momentum equations, which are adequate for simulations of tidal circulation in the shallow waters of the Lower Bay, and it provides for a flexible gridding stategy.

In our application of the model, the Lower Bay is enclosed by four land and four open boundaries (Figures 2a & b). The open boundaries are at the Narrows, at the mouth of the Raritan River from South Amboy to Perth Amboy, along the Sandy Hook to Rockaway Point transect, and at Rockaway Inlet. The land boundaries follow the mean low water 2 m isobath. We have subdivided the interior domain of the Bay into 490 grid elements (Figure 2a). The grid size was refined to about 500 m in the areas of potential sand and gravel mining (Figure 1) and expanded in the areas where the bottom material is mud (Figure 1).

Basic information which must be supplied is a representative mean low water depth for each node and the time variation in surface elevation along all open boundaries. This information is available from the National Ocean Survey in the form of hydrographic charts and harmonic constants for the different tidal constituents. For simplicity, we specified only the semi-diurnal lunar M_2 tide at the open boundaries (Table 1), and we assumed that along an open boundary the tidal elevation is in phase and has a constant amplitude.

Our main objective was to assess the effects of specific bathymetric changes on the tidal circulation and tidal elevations in the Lower Bay. This objective was met by first running the model for several tidal cycles to compute tidal currents (Figures 3a & b) and tidal elevations for existing bathymetry (NOS hydrographic chart No. 12327, 70th Ed., July, 1977).

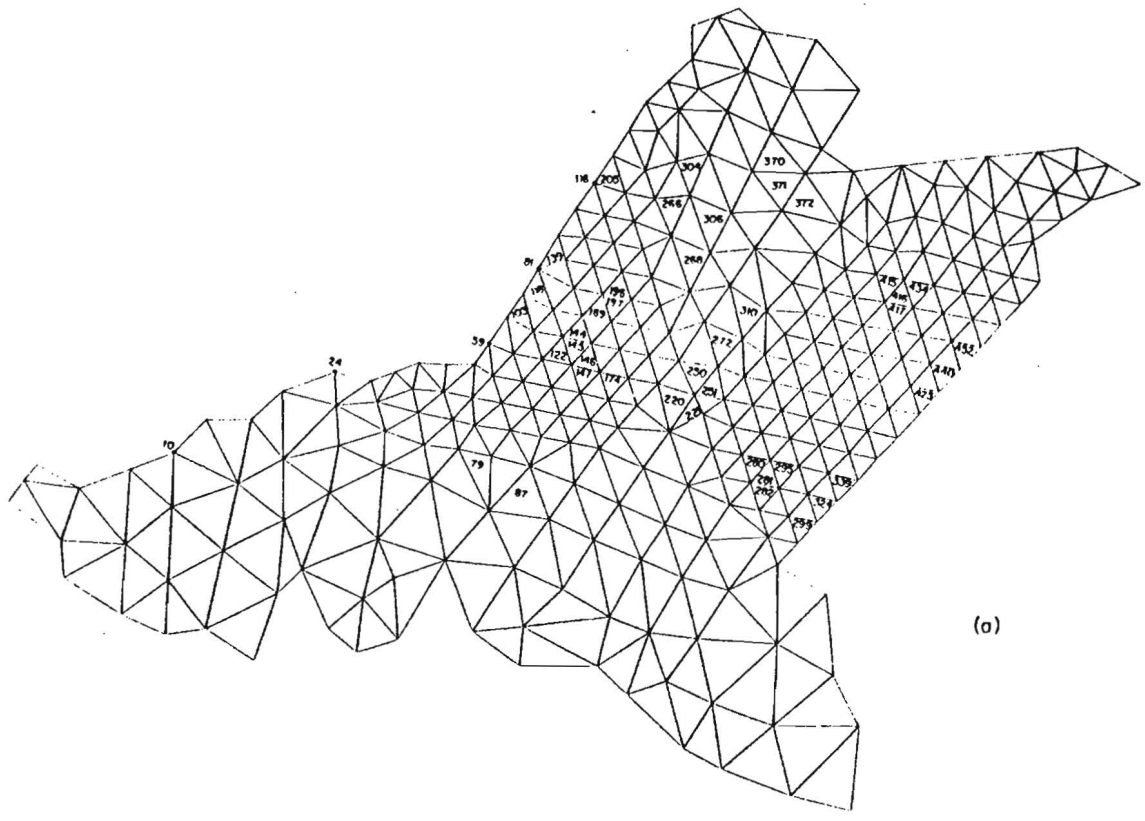

Figure 2a Finite element grid for the Lower Bay of New York Harbor indicating the numbers of selected nodes and elements discussed in text.

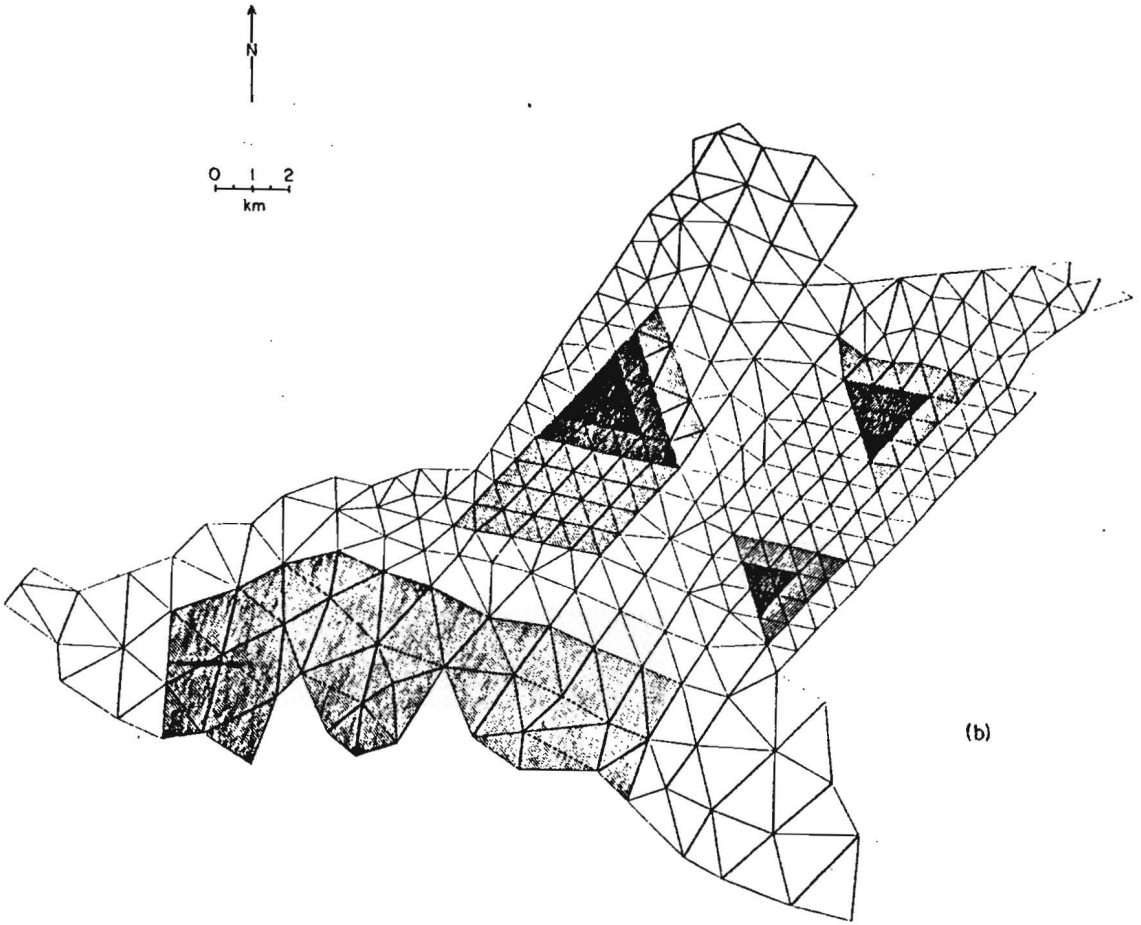

Figure 2b Finite element grid for the Lower Bay of New York Harbor indicating the eight regions of hypothetical mining (shaded).

Figure 3a Computed tidal current vectors for existing bathymetry (NOS hydrographic chart No. 12327, 70th Ed., July 1977) for maximum ebb at Sandy Hook.

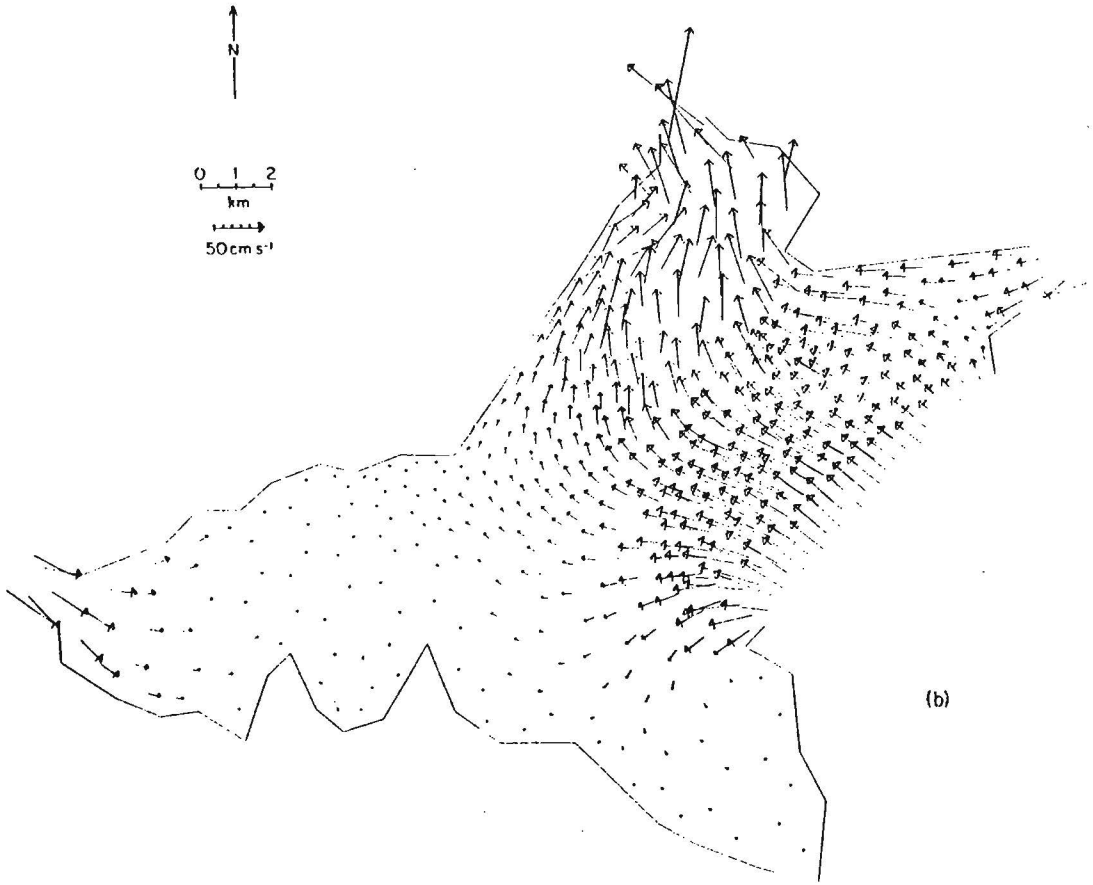

Figure 3b Computed tidal current vectors for existing bathymetry (NOS hydrographic chart No. 12327, 70th Ed., July 1977) for maximum flood at Sandy Hook.

Table 1. Amplitude and phase of M_2 tide specified at the open boundaries.

Boundary	Amplitude (m)	Phase κ (°)
Narrows	0.673	220.7
Perth Amboy - South Amboy	0.737	213.2
Sandy Hook - Rockaway Point	0.676	218.0
Rockaway Inlet	0.737	219.2

The frictional coefficient was adjusted to obtain reasonable agreement between simulated currents and current observations made by the National Ocean Survey and reported by Pritchard, Okubo and Mehr [1962]. Bottom stress terms in the model are in the form

$$\tau_x^b = C_f \rho (q_x^2 + q_y^2)^{\frac{1}{2}} \frac{q_x}{H^2}$$

$$\tau_y^b = C_f \rho (q_x^2 + q_y^2)^{\frac{1}{2}} \frac{q_y}{H^2} \qquad (1)$$

where τ_x^b and τ_y^b are horizontal bottom shear stresses in the x and y directions, q_x and q_y are discharges per unit width, H is the depth, ρ is the density of the water, and $C_f = n^2 g / H^{1/3}$ is the Manning's friction coefficient. We have used a constant value of 0.036 $sm^{-1/3}$ for n, and thus C_f is inversely proportional to $H^{1/3}$. Since our main concern was the tidal circulation, no surface wind stress was applied.

We selected a time step of 40 seconds for the computations in connection with the grid system in Figure 2a. This time step was determined by the Courant-Friedrichs-Lewy Criteria that requires $\Delta t \leq \Delta S / \sqrt{2gH}$ where ΔS is the grid spacing and H is the depth.

Having run the model for several tidal cycles for existing bathymetry, we then ran the model on the same grid for a variety of bathymetric configurations altered to represent the effects of sand and gravel mining activities and compared the results to those from the first run. For eight separate configurations (Figure 2b) we artificially increased the depth to 15 m below mean low water. The depth of 15 m is in keeping with current U.S. Army Corps of Engineer's regulations. Our objective was to assess the importance of both the positioning and the areal extent of the mined region within the Lower Bay. The locations

chosen corresponds to areas of potential sand and gravel mining. This was determined by the geophysical and sedimentalogical studies of Schubel and Fray [Kastens *et al.*, 1978] who have documented the distribution and character of the resource throughout the Lower Bay of New York Harbor (Figure 1).

Figures 4, 5 and 6 provide a comparison of the tidal circulation patterns before and after hypothetical mining at seven of the locations. Solid lines indicate the outline of the hypothetical mining area, dashed arrows indicate current vectors for existing bathymetry, and solid arrows indicate the predicted tidal current vectors after the hypothetical mining to a depth of 15 m below mean low water. We have not presented a comparison for the large hole mined in Raritan Bay; the computed tidal currents in the area for existing bathymetry are quite low, often of the order 5 cm s^{-1}, and the change in currents for the altered bathymetry is at most a few centimeters per second. For selected elements (Figure 2a) we have tabulated the magnitude of current velocities (Table 2) to demonstrate quantitatively the effects of mining.

The tidal elevation above mean low water at each node is also computed by the model. We have examined the effects of mining on tidal range along Staten Island where shore erosion has been a serious problem. Figures 7 and 8 provide a comparison of tidal elevation before and after each of the eight hypothetical mining activities for nodes 10 and 116 (Figure 2a), respectively.

RESULTS

The circulation patterns in Figures 4 through 6 indicate that hypothetical sand and gravel mining activities could change not only the magnitude but also the direction of the currents. All comparisons indicate that the current velocity decreases inside the mined area (the hole) and increases outside the

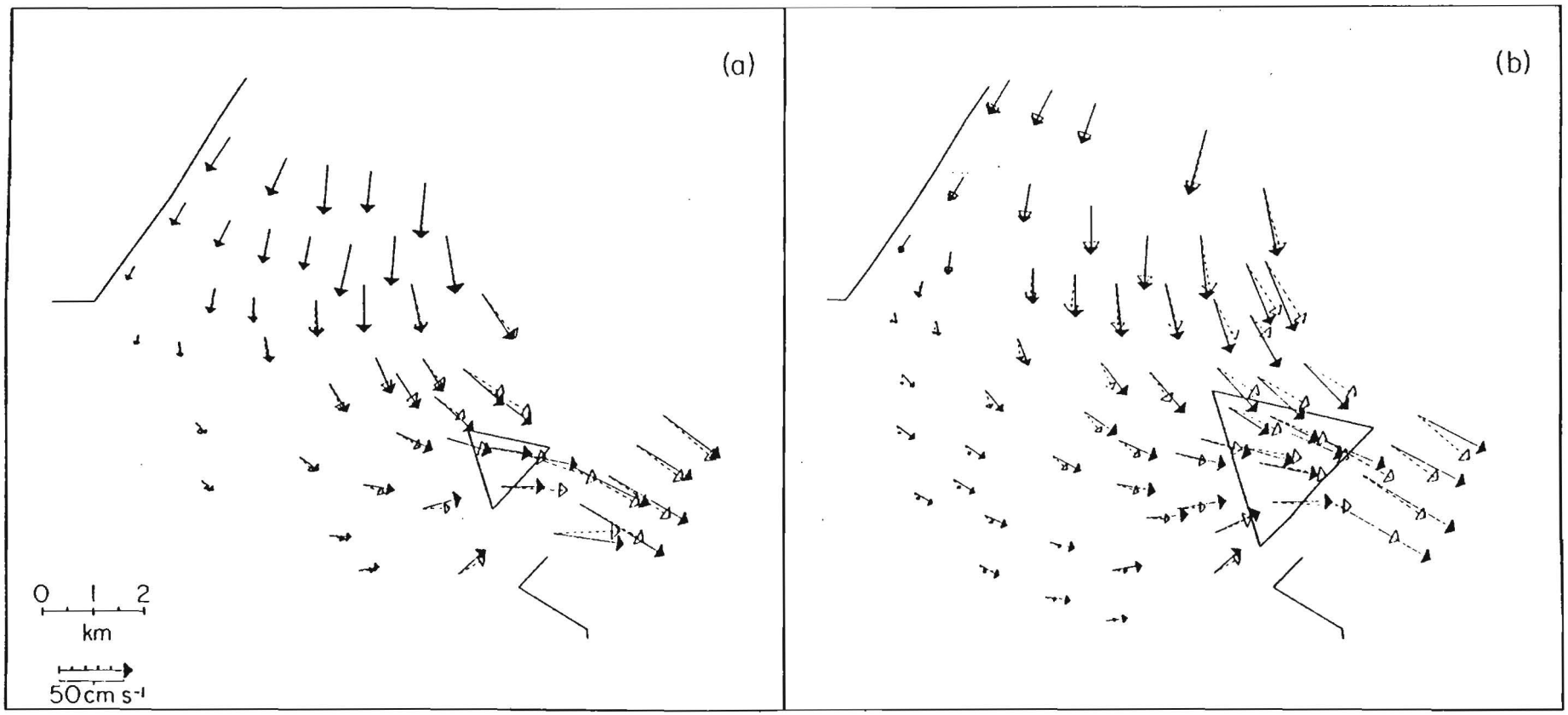

Figure 4 Comparison of tidal current vectors near maximum ebb at Sandy Hook computed for existing bathymetry (dashed arrows) and altered bathymetry (solid arrows) for (a) small region mined near Sandy Hook, (b) large region mined near Sandy Hook (see Figure 2b).

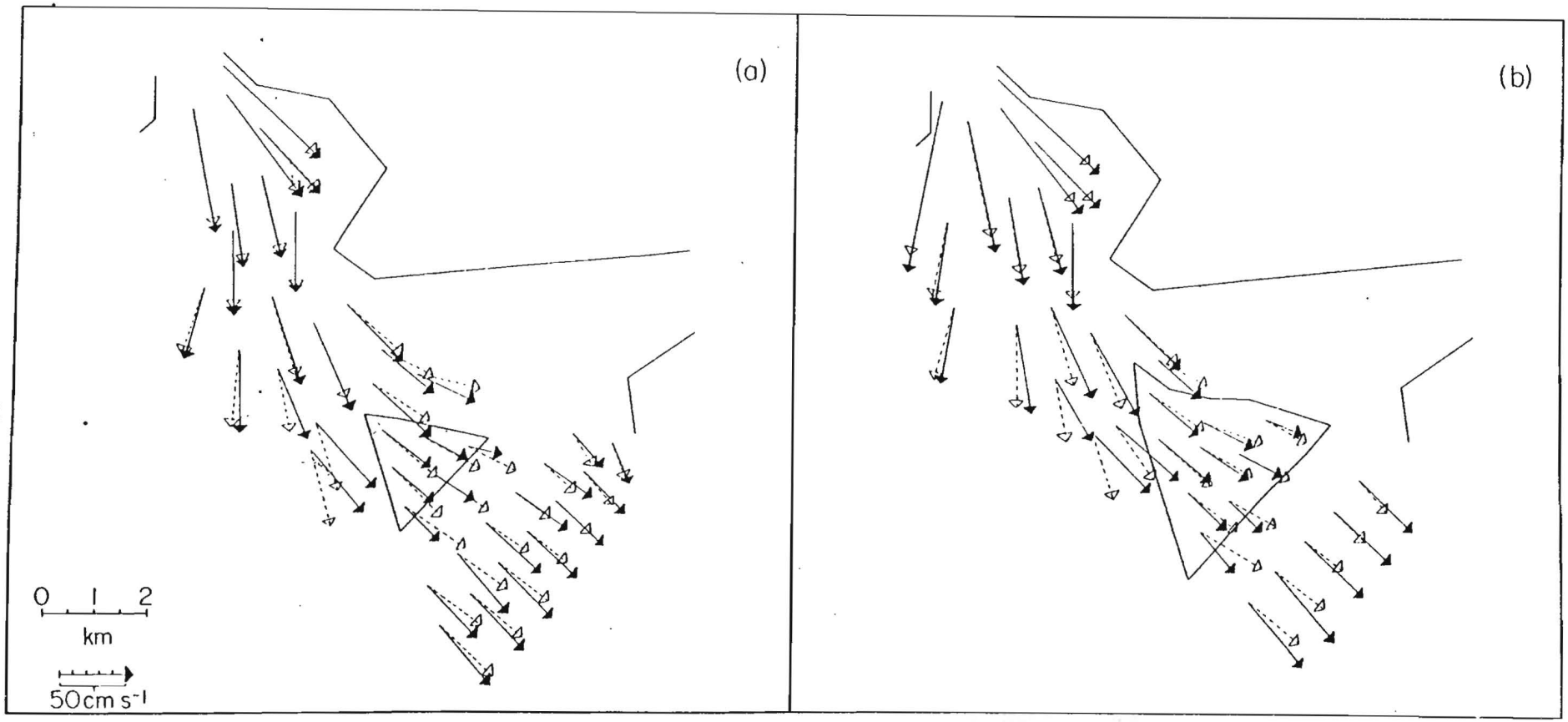

Figure 5 Comparison of tidal current vectors near maximum ebb at Sandy Hook computed for existing bathymetry (dashed arrows) and altered bathymetry (solid arrows) for (a) small region mined near Rockaway Point, (b) large region near Rockaway Point (see Figure 2b).

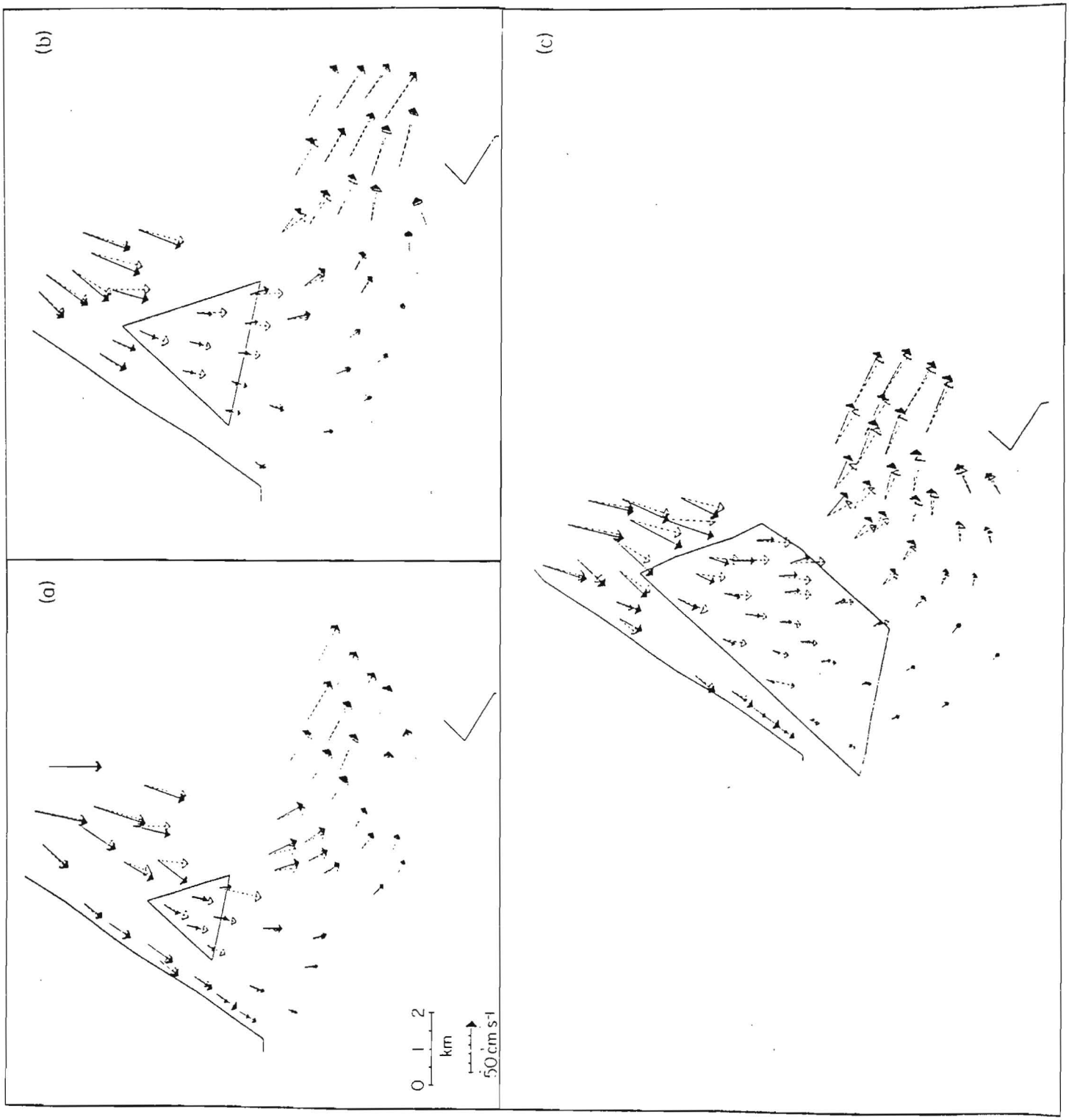

Figure 6 Comparison of tidal current vectors near maximum ebb at Sandy Hook computed for existing bathymetry (dashed arrows) and altered bathymetry (solid arrows) for (a) small region, (b) intermediate size region, (c) very large region mined near Staten Island (see Figure 2b).

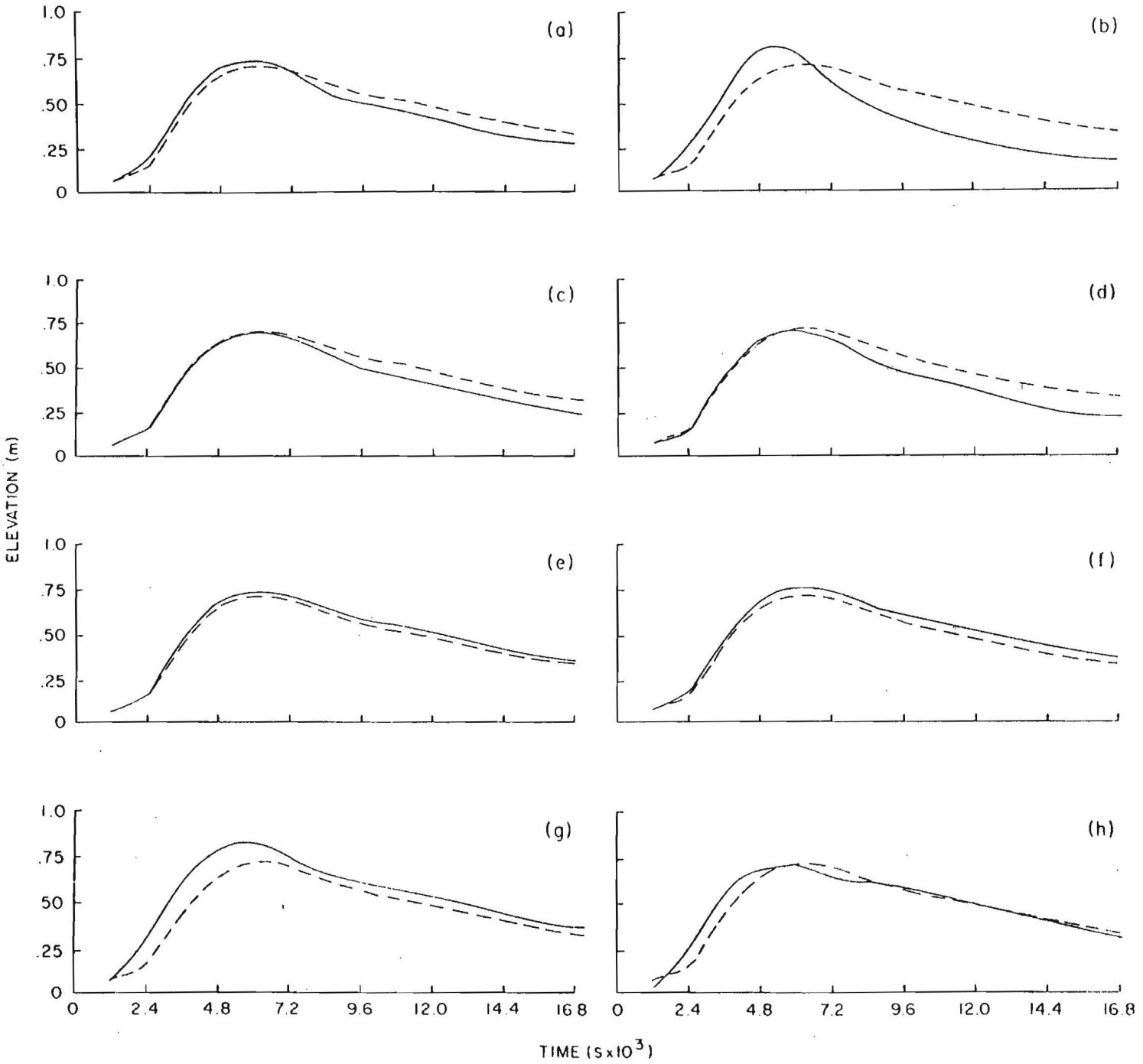

Figure 7 Comparison of tidal elevation along Staten Island at node 10 (Figure 2a) computed for existing bathymetry (dashed lines) and altered bathymetry (solid lines) for (a), (b) small and large region mined near Sandy Hook; (c), (d) small and large region mined near Rockaway Point; (e), (f), (g) small, intermediate and very large region mined near Staten Island; (h) very large region mined in Raritan Bay (see Figure 2b). Tidal datum is discussed in text.

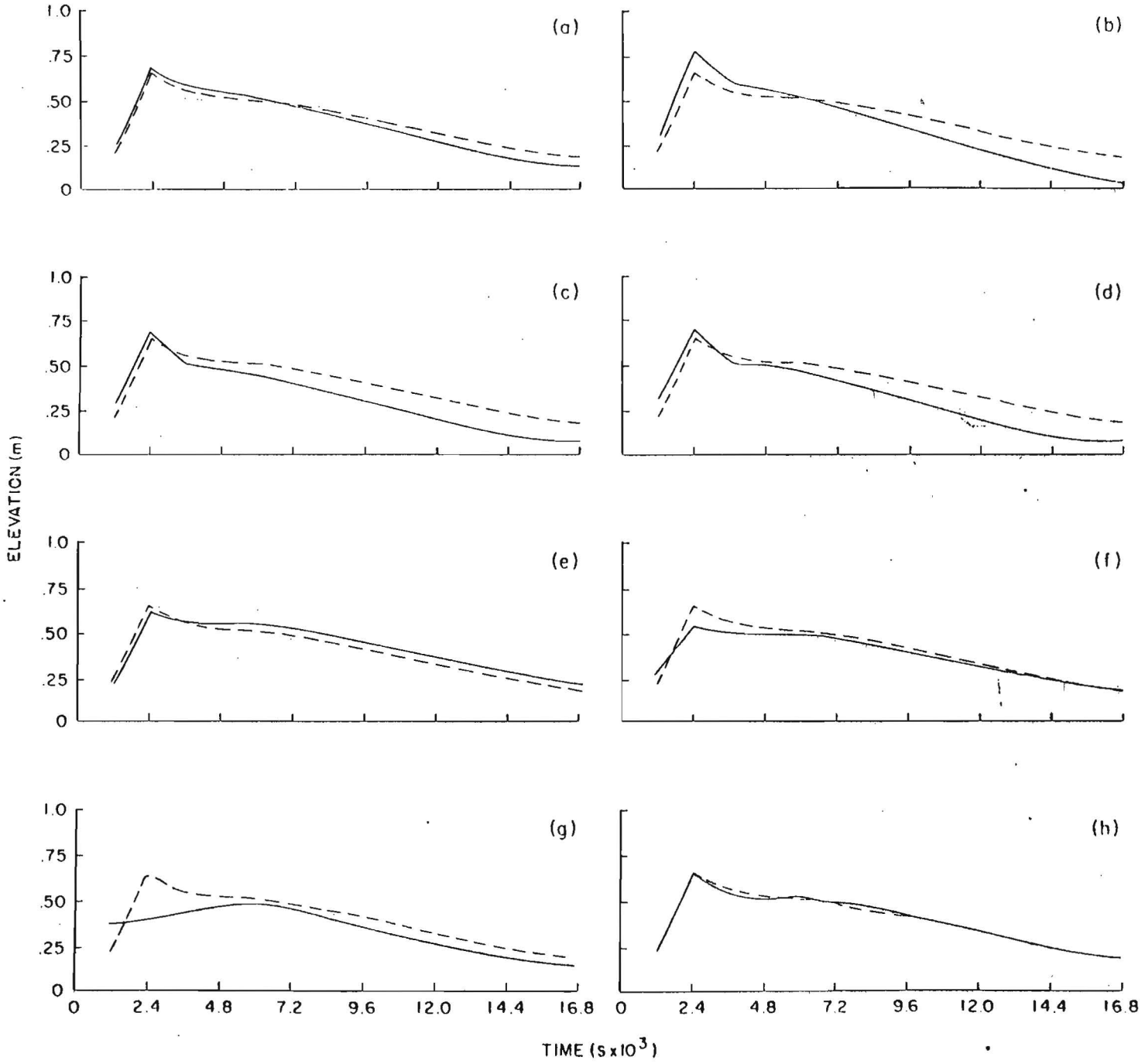

Figure 8 Comparison of tidal elevation along Staten Island at node 116 (Figure 2a) computed for existing bathymetry (dashed lines) and altered bathymetry (solid lines) for (a), (b) small and large region mined near Sandy Hook; (c), (d) small and large region mined near Rockaway Point; (e), (f), (g) small, intermediate and very large region mined near Staten Island; (h) very large region mined in Raritan Bay (see Figure 2b). Tidal datum is discussed in text.

Table 2. Comparison of the magnitude of tidal current vectors for maximum ebb at Sandy Hook computed for existing bathymetry and altered bathymetry. See Figure 2 for relative positioning of elements and mined regions. Abbreviations used below for geographic locations: SH - Sandy Hook, RP - Rockaway Point, SI - Staten Island.

Element Number	280	281	282	295	299	324	339	220	250	272	310
Existing Bathymetry ($cm\ s^{-1}$)	42.0	48.2	48.0	58.8	47.6	52.4	54.2	21.6	28.2	32.8	43.6
Large Hole near SH ($cm\ s^{-1}$)	36.2	41.6	39.4	45.8	53.4	80.8	78.4	30.4	38.2	39.6	47.4
Small Hole near SH ($cm\ s^{-1}$)	30.2	33.6	30.2	35.6	51.6	71.8	68.2	25.8	30.8	34.2	44.2

Element Number	415	416	417	434	423	440	452	370	371	372
Existing Bathymetry ($cm\ s^{-1}$)	44.2	42.8	43.8	40.0	46.2	43.8	32.4	57.6	60.2	59.8
Large Hole near RP ($cm\ s^{-1}$)	42.2	36.0	37.8	33.2	60.8	65.8	58.4	70.6	74.2	70.4
Small Hole near RP ($cm\ s^{-1}$)	32.6	28.8	20.2	25.6	55.6	54.6	47.2	61.8	66.4	59.8

Element Number	169	196	197	266	268	205	147	174
Existing Bathymetry ($cm\ s^{-1}$)	21.8	20.2	20.0	35.8	26.0	20.8	15.6	17.2
Large Hole near SI ($cm\ s^{-1}$)	12.8	13.6	13.6	37.6	26.2	23.8	20.2	21.8
Small Hole near SI ($cm\ s^{-1}$)	11.8	12.6	12.2	37.4	25.2	22.8	18.4	19.6

Element Number	122	144	145	146	304	306	103	118	139	205	221
Existing Bathymetry ($cm\ s^{-1}$)	14.8	14.8	15.4	14.4	43.8	52.8	13.8	15.6	19.8	20.8	22.8
Very Large Hole near SI ($cm\ s^{-1}$)	7.6	7.6	7.8	8.2	54.4	54.2	29.6	23.8	22.2	23.8	25.6

perimeter of the hole. Table 2 suggests that the change in current magnitude can exceed 20 cm s^{-1} and currents may be accelerated over some distance from the hole. Figures 4 through 6 show that upstream of the mined area the flow is deflected towards the hole, and that the deflection increases with the size of the hole. In general, it is clear that a large hole is capable of accelerating currents and changing their direction substantially over some distance from its perimeter, while a smaller hole is more effective in decelerating the currents within its perimeter.

To see why flow towards a hole first accelerates and then decelerates, it is useful to examine the idealized problem of two-dimensional potential flow (no friction) over a semicircular ditch with a uniform flow U_∞ at great distance upstream of the ditch (Figure 9a). Milne-Thomson (1965) derived a relationship between the square of the current magnitude Q^2 and the coaxal coordinates ε and η (Figure 9b) for this flow pattern:

$$Q^2 = \frac{16\, U_\infty^2}{81} \left(\frac{\cosh \eta - \cos \varepsilon}{\cosh \frac{2\eta}{3} - \cos \frac{2\varepsilon}{3}} \right)^2 \qquad (2)$$

By examining Q^2 we can see how the velocity of the flow changes as it approaches the ditch from infinity. At infinity $Q^2 \to U_\infty^2$ (equation 2). As the flow approaches the ditch from upstream, it is no longer uniform; the streamlines are compressed and the speed increases. Two points upstream of the ditch, A' and A" (Figure 9b), have been chosen to demonstrate this situation. From equation (2), Q^2 at A' is 1.12 U_∞^2 and Q^2 at A" is 1.07 U_∞^2. When the flow approaches the edge of the ditch, η becomes very large and from equation (2) $Q^2 \to \frac{16U_\infty^2}{81} e^{\frac{2\eta}{3}}$. The speed can therefore become quite large near the ditch. Once the flow has past over the edge of the ditch, the speed decreases according to equation (2). At the bottom of the ditch ($\eta = 0$, $\varepsilon = 3\pi/2$), for example, the speed of the flow

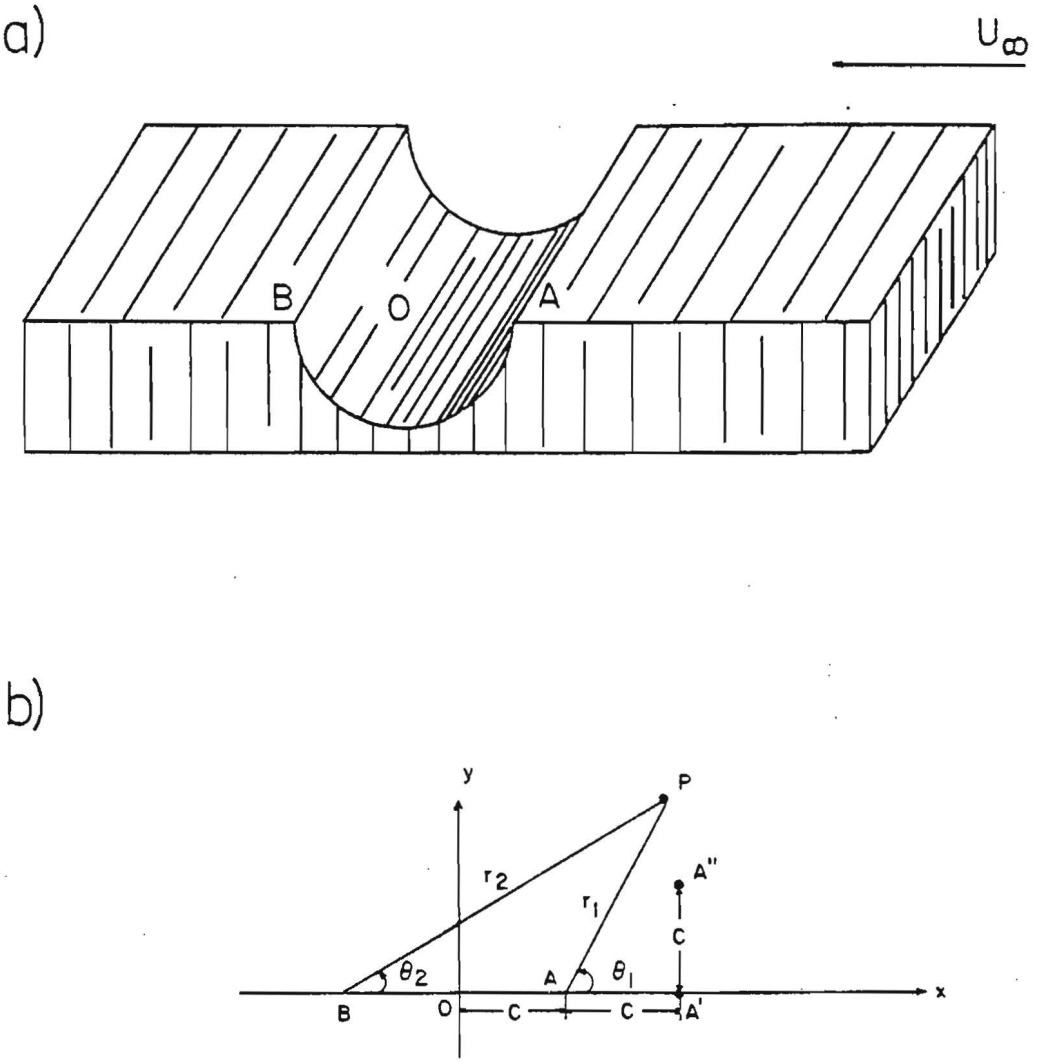

Figure 9 Two-dimensional potential flow past a semicircular ditch (a); coordinate system defining the coaxal coordinate $\varepsilon = \theta_1 - \theta_2$ and $\eta = \ln(r_2/r_1)$ used to describe flow (b) (see text).

is only 0.22 U_∞. Similarly, from equation (2), the flow will be accelerated downstream of the ditch.

This simple case of a two-dimensional potential flow over a ditch is frictionless. In our problem the flow is not frictionless. Larger holes are relatively less effective in decelerating the flow inside their perimeter than smaller holes since bottom stress is reduced over a larger area and the flow tends to accelerate.

In examining the tidal elevation in Figures 7 and 8, it is important to realize that the time scale in both figures extends only to 16800 seconds (approximately ½ tidal cycle) and that approximately the first 6000 seconds are model spin-up. The solid and dashed lines represent tidal elevation above some arbitrary datum; the tide is actually oscillating about mean tide level at some distance above that datum. With this in mind and referring to Figure 7a, for example, we can see that there has actually been an *increase* in tidal amplitude of approximately 6 cm at node 10 for the small hole mined near Sandy Hook.

The results presented in Figures 7a(b) and 8a(b) suggest that mining activity near Sandy Hook could increase the tidal range along Staten Island substantially. The small hole near Sandy Hook will increase the tidal amplitude at node 10 by 6.3 cm and at node 116 by 4.9 cm. The large hole near Sandy Hook will increase the tidal amplitude at node 10 by 15.3 cm and at node 116 by 11.6 cm. Results for mining near Rockaway Point are similar (Figures 7c(d) and 8c(d)). The small hole will increase the tidal amplitude by 7.3 cm and 9.9 cm at nodes 10 and 116, respectively. The large hole will increase the tidal amplitude at node 10 by 10.8 cm and at node 116 by 10.3 cm. This suggests that the tidal range along Staten Island might increase as a result of any increased sand and gravel mining activity near the mouth of the Bay. The degree of increase in tidal range seems to be determined by both the location and the size of the hole.

The effect on tidal range of mining activity near Staten Island (Figures 7e through 7g and 8e through 8g) is much less than that associated with mining near the mouth of the Bay. At node 10 all three holes tend to decrease the tidal amplitude slightly; at node 116 the smallest hole tends to decrease the tidal range, the larger one has little affect, and the largest hole tends to increase the tidal range slightly. The nature of the change in tidal amplitudes at node 116 seems to be determined primarily by the position of the hole. At points near the hole the tidal range increases; at points distant from the hole the tidal ranges decreases. Figures 7h and 8h indicated that the large hole in Raritan Bay has almost no effect on the tidal range along Staten Island.

CONCLUSIONS

It is apparent from the current simulations that increased sand and gravel mining would change the tidal circulation patterns in the Lower Bay. Currents will decelerate within the holes and accelerate outside of them. The water upstream of a hole is deflected towards the hole. Larger holes are more effective in changing the magnitude and direction of the current outside their perimeter while smaller holes are more effective in decelerating the current within the hole.

It is also clear that hypothetical mining near the mouth of the Bay could increase the tidal range along Staten Island substantially; the degree of increase would depend on the location and size of the hole. Mining activity near Staten Island would alter the tidal range slightly and mining within Raritan Bay would have almost no effect on the tidal range along Staten Island.

We can conclude that expanding the sand and gravel mining activities

east of Ambrose Channel and near the mouth of Lower Bay could alter the circulation pattern somewhat. A possibly more important effect, however, would be the substantial increase in tidal range along Staten Island. The effects of mining west of Ambrose Channel would be similar. This increase in tidal range might aggravate the problem of shore erosion along Staten Island; it could, however, have the beneficial effect of improving flushing rates between Raritan Bay and the eastern part of Lower Bay. Mining activities further removed from the vicinity of the mouth of Lower Bay should produce less of an increase in tidal range along Staten Island.

ACKNOWLEDGMENT

This research was supported by the New York Sea Grant Institute through a contract with the New York State Office of General Services, and by SUNY.

NOTATION

C_f	Manning's Frictional Coefficient
g	gravitational acceleration
H	depth
q_x	discharge per unit width in x direction
q_y	discharge per unit width in y direction
Q^2	square of current speed
U_∞	uniform stream at infinity
η, ε	coaxal coordinates, see Figure 9
ρ	density of the water
τ_x^b	bottom shear stress in x direction
τ_y^b	bottom shear stress in y direction
ΔS	grid size
Δt	time increment

Connor, J.J., J.D. Wang, D.A. Briggs and O.S. Madsen. 1973. Mathematical models of the Massachusetts Bay. Ralph M. Parsons Laboratory for Water Resources and Hydrodynamics, Department of Civil Engineering, Massachusetts Institute of Technology, Report No. MITSG 74-4. Index No. 74-304-CbS, 96 pp.

Kastens, K.A., C.T. Fray and J.R. Schubel. 1978. Environmental effects of sand mining in the Lower Bay of New York Harbor: Phase 1. Marine Sciences Research Center, State University of New York at Stony Brook, Special Report 15, Ref. 78-3, 139 pp.

Milne-Thompson, L.M. 1965. Theoretical Hydrodynamics. Macmillan Company, New York, 171-174 p.

Pagenkopf, J.R., G.C. Christodoulou, B.R. Pearce and J.J. Connor. 1976. A user's manual for "CAFE-1": a two-dimensional finite element circulation model. Ralph M. Parsons Laboratory for Water Resources and Hydrodynamics, Department of Civil Engineering, Massachusetts Institute of Technology, Report No. 217, 116 pp.

Pritchard, D.W., A. Okubo and E. Mehr. 1962. A study of the movement and diffusion of an induced contaminant in New York Harbor waters. Chesapeake Bay Institute, The Johns Hopkins University, Technical Report 31, 89 pp.

Wang, J.D. and J.J. Connor. 1975. Mathematical modeling of near coastal circulation. Ralph M. Parsons Laboratory for Water Resources and Hydrodynamics, Department of Civil Engineering, Massachusetts Institute of Technology, Report No. MITSG 75-13, Index No. 75-313-CbS, 272 pp.